LASER INTERFEROMETER GRAVITATIONAL WAVE OBSERVATORY
-LIGO-
CALIFORNIA INSTITUTE OF TECHNOLOGY
MASSACHUSETTS INSTITUTE OF TECHNOLOGY

SURF Final Report **09/07/2001**

Carrier Independent I+ Error Signal Generation Through Addition of Supplementary Antiresonant Amplitude Modulated Sideband

Michael La Marca
Mentor : Dick Gustafson

University of Michigan

California Institute of Technology
LIGO Project - MS 51-33
Pasadena CA 91125
Phone (626) 395-2129
Fax (626) 304-9834
E-mail: info@ligo.caltech.edu

Massachusetts Institute of Technology
LIGO Project - MS 20B-145
Cambridge, MA 01239
Phone (617) 253-4824
Fax (617) 253-7014
E-mail: info@ligo.mit.edu

WWW: http://www.ligo.caltech.edu/

Table of Contents

1. Introduction

These notes are on the generation of a carrier independent error signal for the power-recycling mirror (PRM) of LIGO-like interferometers (long-baseline power-recycled Michelson interferometers coupled with arm Fabry-Perot cavities) through the addition of an amplitude-modulated sideband. This is a variation on the Pound-Drever-Hall technique, which typically uses a phase/frequency-modulated sideband to derive the error signals for LIGO-like interferometers. These notes are intended as a guide to understanding the basics of LIGO-like interferometer control and to provide an insight into a viable alternative control system to the LIGO-Hanford Observatory (LHO).

1.1 Background

This document assumes the reader has a basic knowledge of Fabry-Perot cavities and optics in general. Although the Pound-Drever-Hall technique will be reviewed as it concerns to this project, a basic understanding of it will make this document much more useful. I recommend Eric Black's notes on the topic [1] as well as Ron Drever's original paper [2], both of which are extremely helpful, with Black's paper containing an excellent qualitative, easy to read model of the Pound-Drever-Hall technique. A rudimentary understanding of control systems will also prove helpful. All numbers, frequencies, and data included are based on the LHO 2 kilometer interferometer.

1.2 Motivation

Currently the control system at LIGO utilizes the generation of four linearly independent error signals from the carrier frequency ($\approx 3 * 10^{14}$ Hz) and a phase-modulated sideband offset from the carrier frequency. By beating these two frequencies and utilizing the Pound-Drever-Hall technique, length information can be obtained and error signals generated. The goal of the new system is to provide a cleaner PRM error signal through the addition of an antiresonant amplitude-modulated (AM) sideband to work either as a backup or in conjunction with the current system.

2. Overview Of Cavity Locking and Pound-Drever-Hall Technique

A standard Fabry-Perot cavity consists of two characteristically highly reflecting mirrors facing each other as to reflect a beam between them back and forth. When the mirrors are separated by a distance equal to an integer number of wavelengths of light (or an integer number of free spectral ranges, as these are equivalent conditions), the light reflected between them constructively interferes and a resonance is established. It is highly desirable to maintain this resonance condition and that is what the Pound-Drever-Hall technique does.

To accomplish this, a phase–modulated sideband is added to the carrier beam, usually by a Pockel's cell, that is antiresonant in the cavity when the carrier is resonant. When the carrier is near resonance, a small phase error, representing the small length deviation from resonance (δL), will be seen in the carrier. However, nothing can be done with this error as it resides at an optical frequency many orders of magnitude greater than from which a useable, radio frequency (RF) control/error signal can be derived. Consequently, the carrier is "beat" with the sideband (which

takes place at a nonlinear device, in this case the photodiode), which yields the phase error at the difference frequency between the carrier and sideband. Now the error signal can be extracted at a given difference frequency and used to control the frequency of the laser or operate a length-adjusting servomechanism, although we are only concerned with the latter in our case.

2.1 A Model of Cavity Locking of LIGO-Like Interferometers

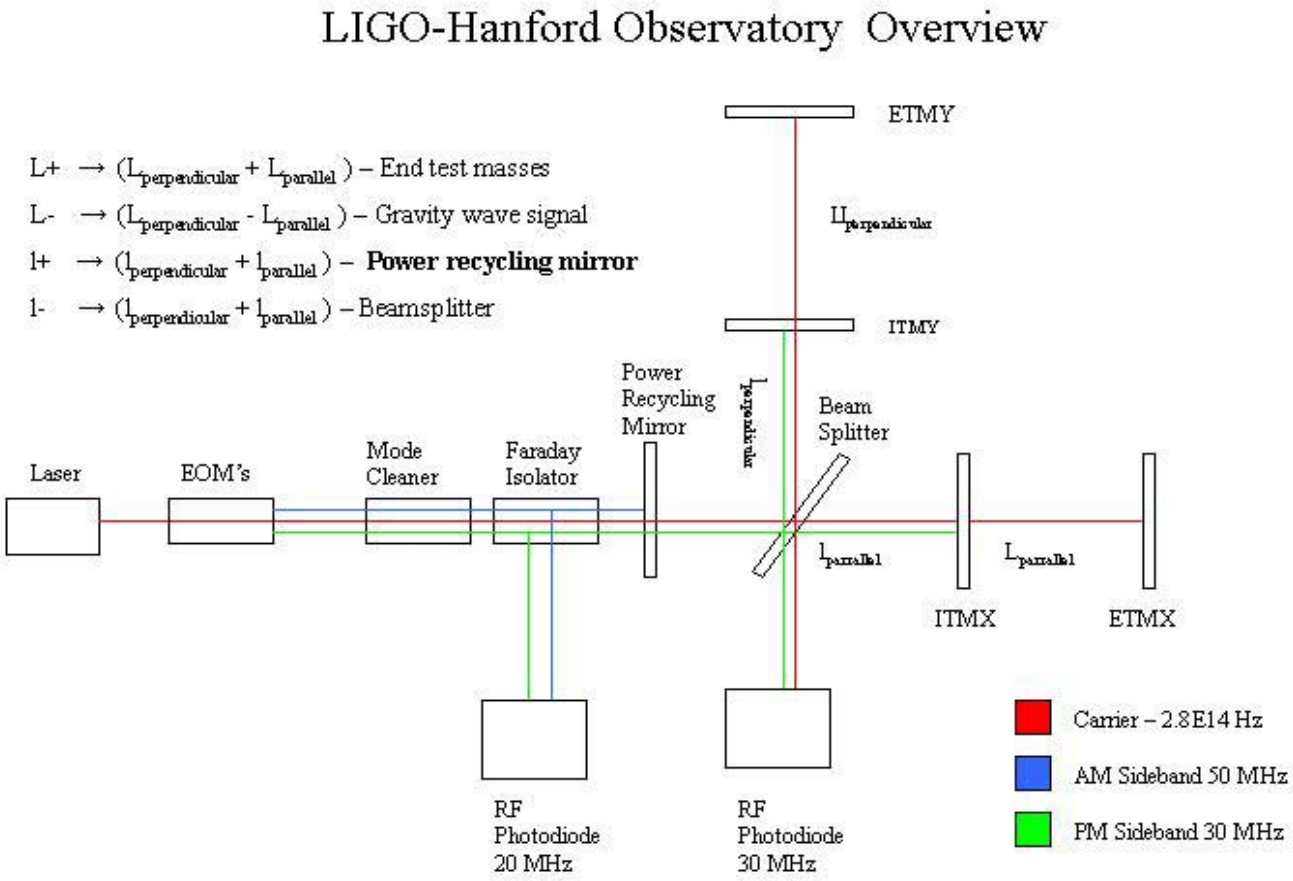

Figure 1

A LIGO-like interferometer consists of three coupled resonant cavities. The first two are those resonant cavities formed between the input and end test masses of the arms and the third is created by inserting a reflecting mirror (power recycling mirror) upstream of the beamsplitter and downstream of the Faraday isolator to form the Michelson cavity, consisting of the power recycling mirror and the two input test masses of the arms (Fig. 1).

To control these three resonant cavities and keep them on resonance, a phase-modulated sideband is added to the carrier that is anti-resonant in the arm cavities but resonant in the Michelson. By beating the carrier and the sideband together at the antisymmetric port, the four

independent error signals controlling the interferometers four degrees of longitudinal freedom can be generated. The error signals consist of the sum and difference of the actual lengths (see Fig. 1) compared to a reference length. The following is a breakdown of each error signal and what it controls:

$L+ \rightarrow (L_{perpendicular} + L_{parallel}) $ – End test masses
$L- \rightarrow (L_{perpendicular} - L_{parallel}) $ – Gravity wave signal
$l+ \rightarrow (l_{perpendicular} + l_{parallel}) $ – **Power recycling mirror**
$l- \rightarrow (l_{perpendicular} + l_{parallel}) $ – Beamsplitter

These error signals are sent to servomechanisms that control the positions of the mirrors to first bring the interferometer into resonance (lock the interferometer) and then keep it there. The actual method for deriving these error signals is beyond the scope of this document but a thorough and excellent account is given in [3] for those who want the full account. The rest of this paper is concerned with an alternate generation of the l+ error signal for the control of the power-recycling mirror.

2.2 Motivation For New Signal Generation

The current control system at LIGO works well and has been proven over time. However, there are difficulties in the system that spawned the need for an alternate way to control the system. First of all, the sideband used to beat against the carrier also contains a phase error, from the small length difference from resonance of the Michelson cavity. Therefore, the carrier, which also contains a phase error from the arm cavities, beats against this sideband to produce an error signal. This mixture of errors degrades the quality of the independent error signals that can be obtained. Another important difficulty is that as the carrier builds up to resonance in the arms, the light transmitted back through the input mirror from the arm cavities (which undergoes a 180-degree phase shift due to the reflection of the light from the end mirror), destructively interferes with the light promptly reflected from the arm cavities. This cavity overcoupling has the effect of causing the error signal to switch signs, and worst of all, disappear at some point during cavity acquisition and locking. We feel our system can either solve or at least ameliorate these problems and most importantly function as a diagnostic tool for both cavity locking and measuring the strength of the resonance in the Michelson cavity.

3. Conceptual Overview

Our project adds another sideband, this one amplitude rather than phase modulated, to the beam. This AM sideband is anti-resonant in the Michelson and arm cavities and is almost totally reflected from the Michelson and arm cavities when the system is near resonance. Therefore, this sideband is “clean”, meaning it does not contain an error in it since it has not entered either of the cavities. Therefore, the phase-modulated sideband has a clean sideband to beat against and we can now obtain a clean, robust independent error signal for the PRM directly from our beat frequency.

3.1 Adding An Amplitude Modulated Sideband

An optical sideband is added to a light beam by passing the polarized light beam through a Pockels cell. A Pockels cell works on the effect of the same name, which changes the index of refraction between the orthogonal axes of an anisotropic crystal when an electric field is applied. This means that the crystal imparts a phase difference between the perpendicular components of a laser beam that passes through the crystal proportional to the electric field across the crystal. The Pockels cell, therefore, can act as a voltage variable phase modulator if a linearly polarized beam (no perpendicular component) is sent through the crystal completely parallel to the active (fast) axis. This is how we generate phase-modulated sidebands (see appendix A).

Generating amplitude-modulated sidebands is more nontrivial. First of all, the beam coming into the Pockels cell must be linearly polarized and aligned at 45 degrees to the crystals active and slow axes for maximal results (Fig. 3).

The Pockel's cell replaces the retarder in this setup and acts as a voltage-variable wave plate (VVWP), with the fast and slow axis at 45 degrees to the input polarization.

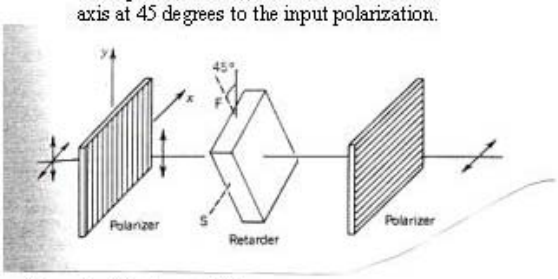

Figure 3 – Courtesy of [4]

Now as before the Pockels cell puts a phase difference between the orthogonal components of the beam based on the applied voltage across the crystal. The Pockels cell is now in reality functioning as a voltage variable wave plate (VVWP), and to complete the system we add a polarizer with its transmission axis perpendicular to the input polarization (the analyzer). By applying a differing voltage to the Pockels cell (VVWP), the amplitude of the laser beams electric field component that passes through the analyzer can be varied (due to the phase shift) and therefore the beam amplitude can be modulated. This can be explained in the following way: The analyzer only transmits the component of the electric field aligned along its transmission axis, regardless of the phase of component in that direction. In the case of phase modulation, there is only one component along one of the axes of the Pockels cell, so even if a polarizer was aligned with an active axis of the Pockels cell (unlike Fig. 3), all of the power would go through since a polarizer cannot distinguish a phase along its transmission axis. However, when there are two components with a phase difference between them as there are after the light passes through the Pockels cell, the two components can add or subtract along the transmission axis depending on the relative phase between them (Fig 3a).

Figure 3a - Time snapshots of electric field components when slow axis component is at maximum depending on phase

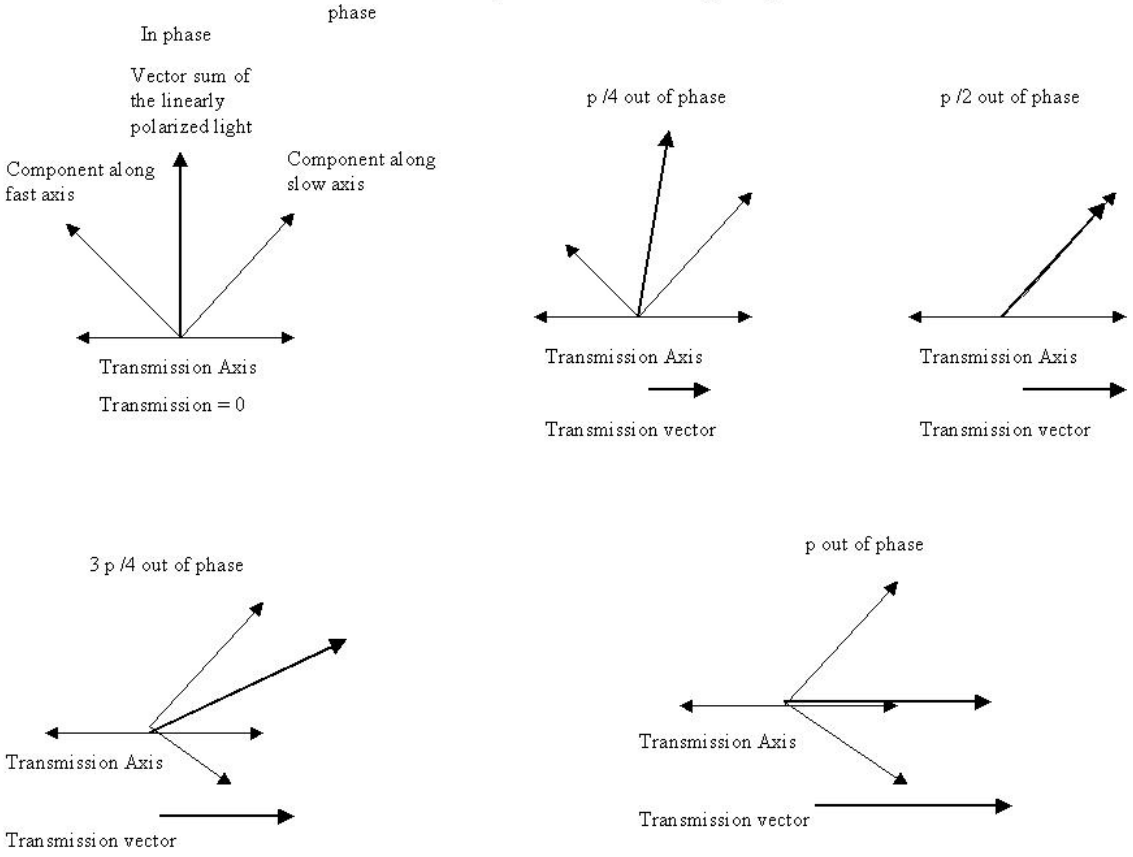

Since this phase difference is directly proportional to the voltage applied across the crystal the amplitude output of the light cannot only be set (as with a direct current), but modulated with an alternating current for modulation frequencies from DC to the hundreds of MHz range. It is important to note that although the phase difference introduces elliptical or circular polarization (Fig. 3b), we are only concerned with the electric field component at a given reference point, in this example when the component orthogonal to the fast axis is at a maximum,

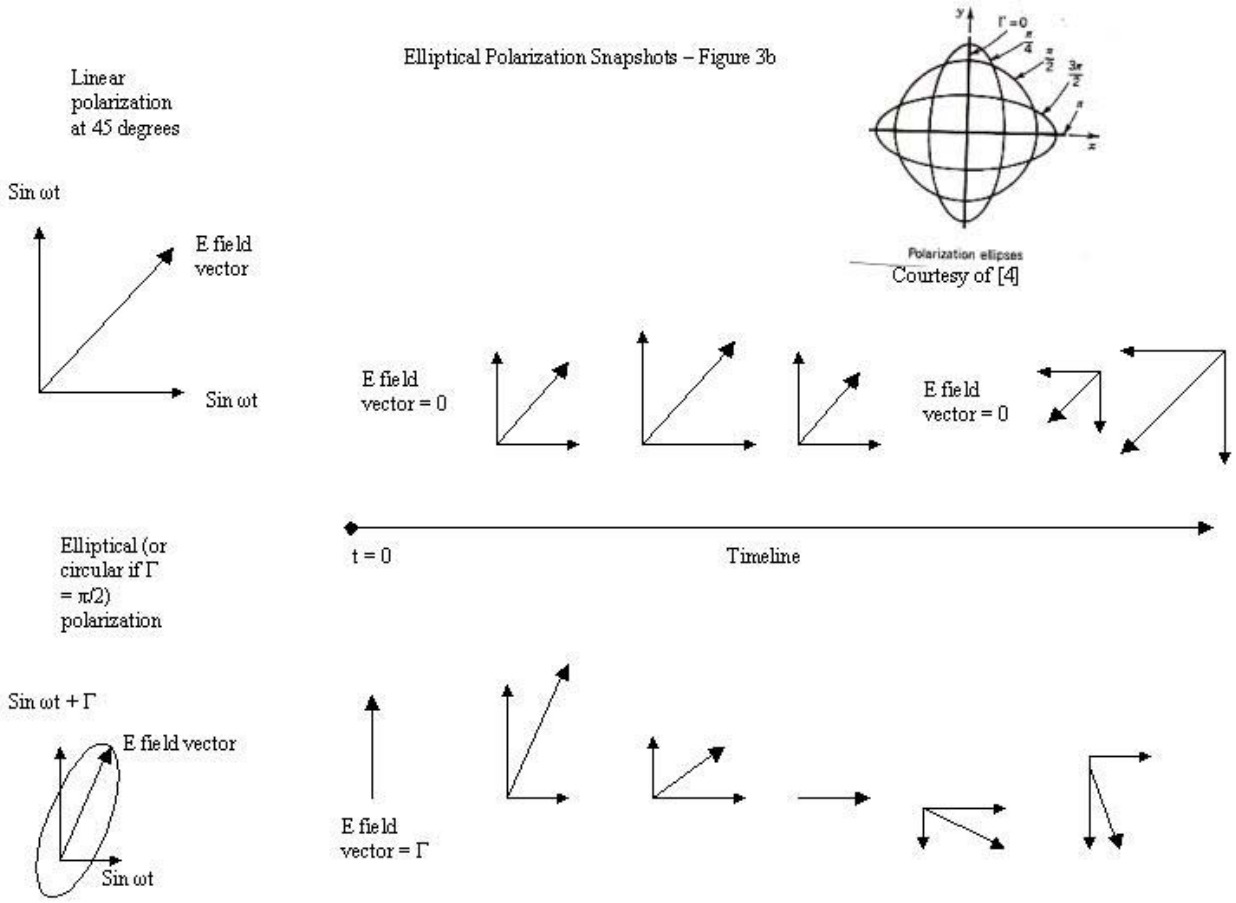

That said, the transmittance of power through the system based on voltage goes like:

$$T(V) = \sin^2\left(\frac{\Gamma_0}{2} + \frac{\pi}{2} * \frac{V}{V_\pi}\right)$$

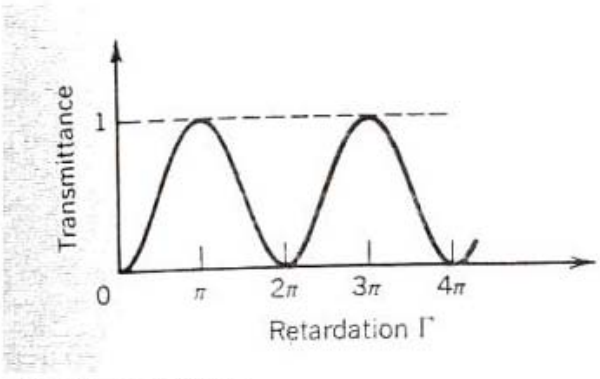

Figure 3c – Courtesy of [4]

where Γ_0 is the initial phase difference in the light and V_π is the voltage needed to produce a phase shift of 180 degrees (half-wave plate).

As you can see (Fig. 3c), when the total retardation is zero the power transmitted is zero and when the voltage equals the half wave voltage (with $\Gamma_0 =$ 0), all the power goes through. If the initial phase difference is set near a $\pi/2$ (quarter wave plate), the modulation enters the linear regime, and this is accomplished through a constant bias voltage or a quarter-wave plate. A linear relation between driving voltage and power transmittance is important so as to achieve a proportional correspondence between the driving waveform and the output power waveform. The mathematical description of amplitude modulated sideband generation is in appendix A.

3.2 Phase vs. Amplitude Modulation

An important aspect of both amplitude and phase modulation is that both add sidebands at the carrier frequency plus or minus the driving frequency. (Although phase modulation adds sidebands at harmonics of the driving frequency as well as the driving frequency, these higher order sidebands usually having negligible amplitude). A natural question that comes to mind is why one AM sideband and one PM sideband instead of just 2 PM sidebands? The answer to this question is contained in appendix B, where it can be shown that 2 PM sidebands cancel out any error signal, and are therefore useless, while an AM sideband and a PM sideband beat to produce an error signal (Appendix C).

3.3 Error Signal Generation

When a Fabry-Perot cavity is not on resonance ("locked"), the reflected light from the cavity obtains an error in the form of a small phase shift, represented by $2k\Delta L$, with ΔL being a small length deviation from resonance and the wave number $k = 2\pi/\lambda$. This is the cornerstone of the Pound-Drever-Hall system for maintaining a cavity on resonance. We take this concept one step further by using two sidebands to obtain the error instead of a carrier and a sideband. The rest of the process is actually very similar. The beating, or combination of two different optical frequencies to produce their frequency difference, of the two sidebands actually occurs on the photodiode, which converts the light power, not electric field, into a voltage. Because we can only see radio frequencies (up to 125 MHz in our case) from the photodiode, it is impossible to look specifically at the sideband containing the error, which is at a frequency of 10^{14} Hz. Therefore, we beat the two sidebands together, and their difference frequency contains the error term. Since the sidebands are offset from the carrier by their modulation frequency, it is trivial to determine the beat frequency to look at, as it is only the difference in the modulation frequencies of the sidebands. However, it is nontrivial to actually look at that frequency, as the signal coming from the photodiode is composed of a variety of different frequencies. To extract the beat frequency containing the error, we pass our signal through a mixer, a nonlinear RF device that, with filtering, can pick out the component of the signal with the same frequency that drives the mixer at. If we drive the mixer at the beat frequency and input the photodiode signal, we can obtain the error signal audio frequencies. By sending this audio error signal to a servomechanism, we can control the position of a mirror and keep the cavity on resonance. An important note is that the sign of the error signal changes depending on which side of resonance (too short or too long) you are on ($\pm\Delta L$ gives you a positive or negative control signal) and that the error signal is zero when the cavity is on resonance. From a control systems perspective, those are exactly the characteristics you would like your error signal to have. A complete mathematical work-up showing the beating of a PM and AM sideband and the actual derivation for the error signal term is provided in Appendix C.

4. Actual Project

This is a description of the actual optical and electrical setup we used, which although is similar to the theoretical description, was altered to correct and/or upgrade the difficulties one encounters when leaving the theoretical and entering the experimental realm.

4.1 Project Apparatus

The apparatus used to produce the AM sidebands was remarkably similar to the conceptual model of one. Our apparatus consists of a half-wave plate (the light is already linearly polarized in the vertical direction by the laser), the Pockel's cell (Newport model 4104) with crystals aligned 45 degrees to the input polarization, two wedges, an antireflective window, and a polarizing beam splitter, which functioned as the analyzer. The wedges and antireflective window were used to correct for the Pockel's cell (electro-optic modulator/EOM), which displaced and bent the output beam by approximately 1 mm and 1 degree respectively. Matching feet were placed on the apparatus and on the PSL optical table so that the apparatus could restored to a position within 50 microns each time it was swapped in and out of the beam path in order to maintain excellent alignment with the mode cleaner.

A difficulty with amplitude modulation is that to be in the linear regime, one must have a transmittance of around half, as mentioned before. Unfortunately, LIGO requires all the power of the laser to be utilized in the system in order to increase sensitivity. Therefore, half power dissipation is not an option. We accounted for this by putting the analyzer's transmission axis parallel rather than perpendicular to the input polarization, which turns the transmittance from a $\sin^2$ to a $\cos^2$ function, meaning that at zero voltage we had full power transmittance. We then drove our EOM with a bias voltage enough to put us around the 90 percent transmittance mark. Our modulation depth of 5 percent (10 percent peak-to-peak) of the output voltage resulted in a uniform correspondence between driving and output waveform, although the parallel alignment of the polarizer and analyzer introduces a 180-degree phase shift between the driving waveform and the output power waveform.

4.2 Frequency Decisions

For the 2k interferometer, we chose the frequency of 49.179402 MHz to modulate the EOM at. This frequency correlated to a multiple of the mode cleaner's free spectral range and was not an integer multiple of the phase modulated sideband at 29.507642 MHz so that it would pass through the mode cleaner and have minimal interference with the PM sideband. It also avoided the resonances of the arm cavities and the Michelson cavity and was less than 70 MHz, thereby conforming to the specifications of an anti-resonant sideband as given in the Input Optics Final Design parameters [5]. Therefore, our error signal is at a beat frequency of 19.67176 MHz.

4.3 Error Signal Extraction

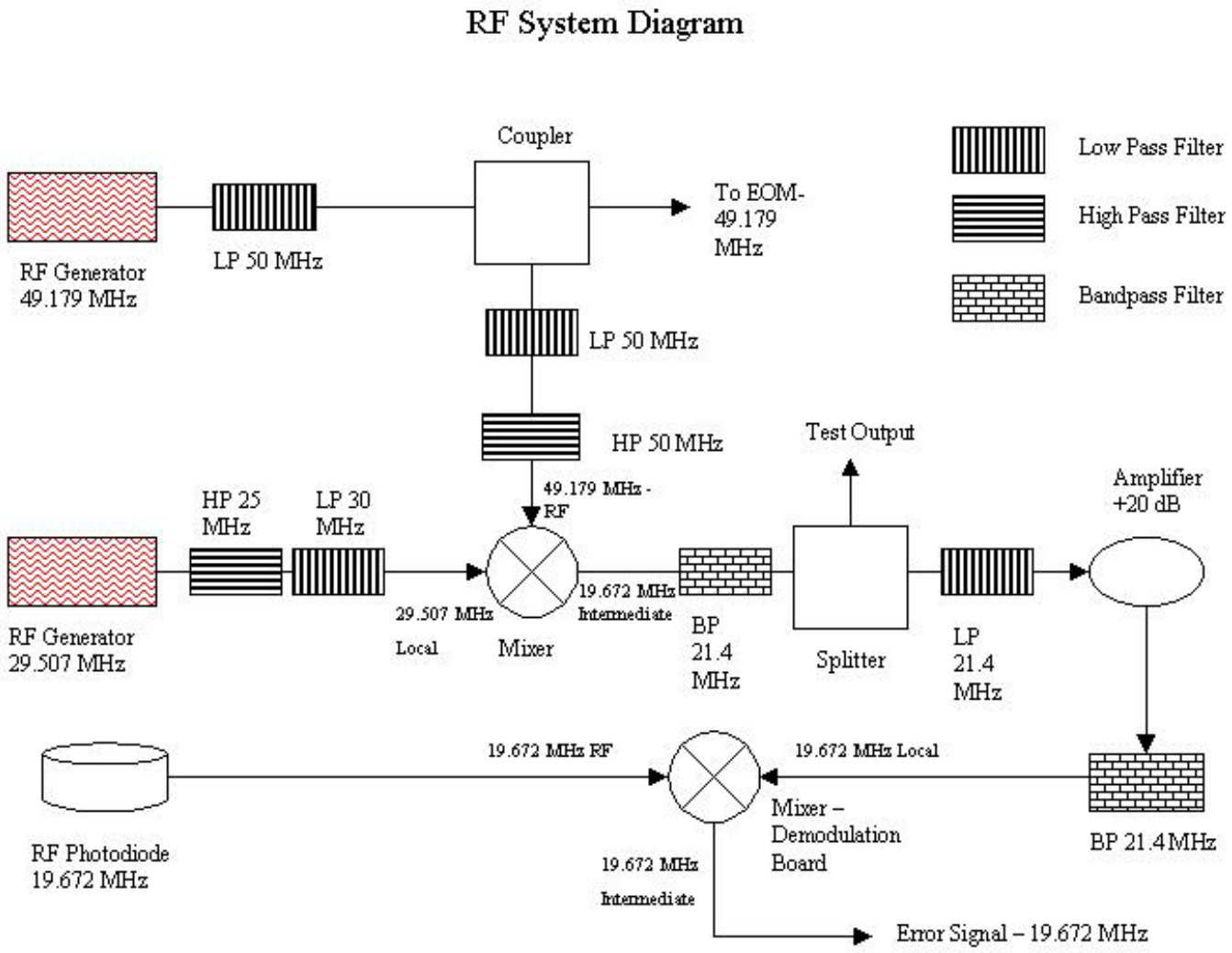

Figure 4

To obtain an error signal the equipment was first modified to accommodate our specific frequencies. A resonant circuit was built to amplify the voltage sent to the EOM due to its very high voltage requirements even for small retardation levels. The photodiode was retuned to 19.67167 to select and amplify our beat frequency. From Fig. 4, one can see that we mix signals twice to demodulate our final error signal. Our EOM driving frequency is split and sent into the first mixer as an RF signal. The local oscillator signal to this mixer comes from PM sideband RF signal generator at 29.507642 MHz and the output is selected to be the 19.67167 MHz beat signal. It is important that this is a clean signal because it becomes the local oscillator signal to

mix with RF photodiode signal. The output of this second mixer contains the error term, which can be on a sine or cosine term of the same frequency. The proper term is selected by modifying the phase of the signal (sine and cosine differ by a $\pi/2$ phase difference), usually by modifying cable lengths.

The filters, consisting of low pass, high pass, and bandpass, are used to selectively pass only the desired frequencies and reduce other RF signals in order to achieve the cleanest signal possible. For example, the mixers will pass the frequencies of the RF signal, the local oscillator signal, and their sum and difference frequencies plus the harmonics. To select a desired signal, the other signals are simply filtered out and then the desired signal is amplified. In our first mixer, we select the difference frequency while in the second mixer (contained in the demodulation board) we select the local oscillator signal, both selected through the use of a combination of different filters tested for maximum signal strength and cleanliness. We have successfully sent our frequency sideband through the mode cleaner, mixed the signals, and obtained a signal at our beat frequency of 19.67167 MHz. This represents the new l+ error control signal for the PRM.

5. Problems, Remaining Hurdles, and Successes

5.1 Problems

Our first problem is that our amplitude modulator at best will reduce the power by ten percent. However, we were noticing power reductions on the order of 40%, which in a worst-case scenario means the optics are losing on the order of 30% of the light. This could be fixed with better optics but at this time we would like to rule out other possibilities before making such an investment. Also, a great difficulty was found in aligning the beam onto the mode cleaner, given the condition of the beam on output from the EOM. The displacement and divergence by a degree of the beam represented two degrees of freedom that had to be corrected for. The wedges were used to steer the beam back to true and the window was placed at an angle in an effort to "walk" the beam back onto the correct path. This represents another problem as each new optic added to the beam path reduces its power through losses. Finally, and perhaps our most distressing problem, was the beam distortion after it went through our apparatus. The outgoing beam was very distorted and most of its power was killed by the mode cleaner, resulting in a weaker beam and therefore signal passing through the mode cleaner, which would not lock on the "trashy" beam. We believe the distortion to be introduced by the EOM and believe that better alignment using a beam scan could possibly correct it.

5.2 Remaining Hurdles

Besides solving the above-mentioned problems, we still have the major hurdle of taking the beat frequency RF error signal and implementing that into the overall LIGO control system architecture to form the audio error signal to be fed to the actuator heads on the power-recycling mirror. After this come the critical tasks of locking the Michelson cavity and the final goal of locking the interferometer using the new error signal. Also, tests will then have to be performed to determine if our signal will lock the interferometer faster, maintain lock longer, and provide

better sensitivity than the current system, in which case it is possible the old system prevails in these criteria. However, at worst we have created an alternate control signal to assist the old control system, and our system has been previously proven to work at locking the interferometer at Caltech' s 40-meter lab.

5.3 Successes

Despite the considerable difficulties left to overcome, much was accomplished. A designated-frequency sideband was created and passed it through the mode cleaner. We constructed and tuned a resonant circuit and a RF photodiode with respectable Q's at their desired frequencies. Our apparatus is completely removable and can be inserted again without the need for realignment, a very useful characteristic given the amount of different experiments and data acquisition that rely on a near-perfect alignment. Despite a non-TEM_{00} beam spot, we passed the beam through the mode cleaner and aligned on the RF photodiode. Most importantly, we constructed the error signal generation system and can extract the 19.67167 frequency signal. Our hope is that with continued effort, our new l+ control signal will be implemented into the system and used to lock and maintain the lock of the interferometer faster, longer, and better than the current system.

Appendix A – AM and PM Sideband Generation

Amplitude Modulation

Input Beam (electric field) to Pockel's cell/EOM

$E = A\sin\omega t$

Beam now gains time - dependent amplitude function

$E = A(t)\sin\omega t$

Chose function to be a sine wave with amplitude M and frequency γ

$E = (I + M\sin\gamma t)\sin\omega t \Rightarrow$ I is an offset index to keep A greater than 0 - let I = 1

Result : Carrier plus sidebands with frequency $\omega \pm \gamma$

$$E = \sin\omega t + \frac{M}{2}\cos((\omega-\gamma)t) - \frac{M}{2}\cos((\omega+\gamma)t)$$

Phase Modulation

Input beam (electric field) to Pockel's cell/EOM

$E_{in} = E_o e^{i\omega t}$

Beam now gains time - dependent phase difference

$E = E_o e^{i(\omega t+\phi(t))}$

Choose function to be sine wave with amplitude β and frequency Ω

$E = E_o e^{i(\omega t+\beta\sin\Omega t)}$

Ignore higher (2nd+) order sidebands - negligible amplitude

$E \approx E_o[J_0(\beta) + 2iJ_1(\beta)\sin(\Omega t)]e^{i\omega t}$

Expand and regroup terms - carrier plus sidebands with frequency $\omega \pm \Omega$

$E = E_o[J_0(\beta)e^{i\omega t} + J_1(\beta)e^{i(\omega+\Omega)t} - J_1(\beta)e^{i(\omega-\Omega)t}]$

The important result to notice is that both phase and amplitude modulation result in a pair (for phase higher order sidebands as well but we ignore them) of sidebands offset from the carrier at plus or minus the driving frequency. The amplitude of these sidebands is dependent on the modulation depth and is not as significant to the error signal generation as the frequency of these sidebands.

Appendix B – Error Signal Vanishing With 2 PM Sidebands

Input beam (Electric field) to Pockels Cell

$E_{in} = E_o e^{i\omega t}$

Beam after first Pockels cell - Approximate using carrier and first order sidebands

$E = E_o e^{i(\omega t + \beta \sin \Omega t)} = E_o[J_0(\beta)e^{i\omega t} + J_1(\beta)e^{i(\omega+\Omega)t} - J_1(\beta)e^{i(\omega-\Omega)t}]$

Beam after second Pockels cell

$E_o[J_0(\beta)e^{i(\omega t+\Gamma \sin \gamma t)} + J_1(\beta)e^{i[(\omega+\Omega)t+\Gamma \sin \gamma t]} - J_1(\beta)e^{i[(\omega-\Omega)t+\Gamma \sin \gamma t]}]$

Ignore sidebands on sidebands - I expressed it this way to emphasize the offset of the sidebands at the modulation frequency from the carrier frequency

$E = E_o[J_0(\beta)\{J_0(\Gamma)e^{i\omega t} + J_1(\Gamma)e^{i(\omega+\gamma)t} - J_1(\Gamma)e^{i(\omega-\gamma)t}\} + J_1(\beta)\{J_0(\Gamma)e^{i(\omega+\Omega)t} - J_0(\Gamma)e^{i(\omega-\Omega)t}\}]$

Introduce an error to Ω sideband, $\phi = 2k(\Delta L)$ where ΔL is a small deviation from the operating point and wavenumber $k = \frac{2\pi}{\lambda}$

$E = E_o[J_0(\beta)\{J_0(\Gamma)e^{i\omega t} + J_1(\Gamma)e^{i(\omega+\gamma)t} - J_1(\Gamma)e^{i(\omega-\gamma)t}\} + J_1(\beta)\{J_0(\Gamma)e^{i((\omega+\Omega)t+\phi)} - J_0(\Gamma)e^{i((\omega-\Omega)t+\phi)}\}]$

We can only look at power in the beam through the photodiode, not electric field amplitude. Since $P = E^2$, we look at the electric field squared. We also must look at frequencies in the RF realm. Optical frequencies cannot be seen as an RF signal so we can discard terms at the optical frequency ω. However, we can observe the "beat" between two optical frequencies and determine an error signal from that. Therefore, I will only include terms with the addition or subtraction of the modulation frequencies.

$P = P_o[J_0(\beta)\{J_0(\Gamma)e^{i\omega t} + J_1(\Gamma)e^{i(\omega+\gamma)t} - J_1(\Gamma)e^{i(\omega-\gamma)t}\} + J_1(\beta)\{J_0(\Gamma)e^{i((\omega+\Omega)t+\phi)} - J_0(\Gamma)e^{i((\omega-\Omega)t+\phi)}\}]^2$

$P = P_o[J_1(\beta)J_0(\Gamma)\{e^{i(\omega+\Omega+\phi)t} - e^{i(\omega-\Omega+\phi)t}\} + J_0(\beta)J_1(\Gamma)\{e^{i(\omega+\gamma)t} - e^{i(\omega-\gamma)t}\}]^2$

$P = P_\omega J_0(\beta)J_0(\Gamma)J_1(\beta)J_1(\Gamma)[e^{i(2\omega+\Omega+\gamma+\phi)t} - e^{i(2\omega+\Omega-\gamma+\phi)t} - e^{i(2\omega-\Omega+\gamma+\phi)t} + e^{i(2\omega-\Omega-\gamma+\phi)t}]$

Factor out $e^{i2\omega t}$ term, does not affect RF signal

$P = P_\omega J_0(\beta)J_0(\Gamma)J_1(\beta)J_1(\Gamma)[e^{i(\Omega+\gamma+\phi)t} - e^{i(\Omega-\gamma+\phi)t} - e^{-i(\Omega-\gamma-\phi)t} + e^{-i(\Omega+\gamma-\phi)t}]$

Taking the real part since strictly speaking $P = [\mathrm{Re}\{E\}]^2$

$P = P_\omega J_0(\beta)J_0(\Gamma)J_1(\beta)J_1(\Gamma)\,\mathrm{Re}[e^{i(\Omega+\gamma+\phi)t} - e^{i(\Omega-\gamma+\phi)t} - e^{-i(\Omega-\gamma-\phi)t} + e^{-i(\Omega+\gamma-\phi)t}]$

$P = P_\omega J_0(\beta)J_0(\Gamma)J_1(\beta)J_1(\Gamma)[\cos(\Omega+\gamma+\phi) + \cos(\Omega+\gamma-\phi) - \cos(\Omega-\gamma+\phi) - \cos(\Omega-\gamma-\phi)\}$

$\cos(\alpha \pm \beta) = \cos\alpha \cos\beta \,\mu\, \sin\alpha \sin\beta$ – Small angle approximation - $\cos\delta = 1$

$P = P_\omega J_0(\beta)J_0(\Gamma)J_1(\beta)J_1(\Gamma)[\{\cos(\Omega+\gamma)\cos(\phi) - \sin(\Omega+\gamma)\sin(\phi) + \cos(\Omega+\gamma)\cos(\phi) + \sin(\Omega+\gamma)\sin(\phi)\}$

$-\{\cos(\Omega-\gamma)\cos(\phi) - \sin(\Omega+\gamma)\sin(\phi) + \cos(\Omega+\gamma)\cos(\phi) + \sin(\Omega+\gamma)\sin(\phi)\}]$

Sin terms cancel out

$P = P_\omega J_0(\beta)J_0(\Gamma)J_1(\beta)J_1(\Gamma)[2\cos(\Omega+\gamma) - 2\cos(\Omega-\gamma)]$

As you can see, our final photodiode (power) output does not contain a term with the error on it because the "beat terms" cancel each other out. This is why we must use one amplitude and one phase modulated sideband.

Appendix C – Error Signal Generation with AM and PM Sidebands

Beam after phase modulation - take to be a sine wave

$$E \approx \mathrm{Im}\{E_o[J_0(\beta)e^{i\omega t} + J_1(\beta)e^{i(\omega+\Omega)t} - J_1(\beta)e^{i(\omega-\Omega)t}]\} \approx E_o[\sin(\omega t) + J_1(\beta)\sin((\omega+\Omega)t) - J_1(\beta)\sin((\omega-\Omega)t)]$$

Beam after amplitude modulation - assume no sidebands on sidebands

$$E = \sin\omega t + \frac{M}{2}\cos((\omega-\gamma)t) - \frac{M}{2}\cos((\omega+\gamma)t) + J_1(\beta)\sin((\omega+\Omega)t) - J_1(\beta)\sin((\omega-\Omega)t)$$

Introduce phase error on PM sideband - $\phi = 2k\Delta L$

$$E = E_o[\sin\omega t + \frac{M}{2}\cos((\omega-\gamma)t) - \frac{M}{2}\cos((\omega+\gamma)t) + J_1(\beta)\sin((\omega+\Omega+\phi)t) - J_1(\beta)\sin((\omega-\Omega+\phi)t)]$$

Power conversion and beating on photodiode

$$P = |E|^2 = P_o[\sin\omega t + \frac{M}{2}\cos((\omega-\gamma)t) - \frac{M}{2}\cos((\omega+\gamma)t) + J_1(\beta)\sin((\omega+\Omega)t+\phi) - J_1(\beta)\sin((\omega-\Omega)t+\phi)]^2$$

Look at cross terms in power expansion - ignore $2\,\Omega/\gamma$ terms

$$P \approx -J_1(\beta)\sin((\omega+\Omega)t+\phi)\frac{M}{2}\cos((\omega+\gamma)t) + J_1(\beta)\sin((\omega+\Omega)t+\phi)\frac{M}{2}\cos((\omega-\gamma)t)$$

$$+ J_1(\beta)\sin((\omega-\Omega)t+\phi)\frac{M}{2}\cos((\omega+\gamma)t) - J_1(\beta)\sin((\omega-\Omega)t+\phi)\frac{M}{2}\cos((\omega-\gamma)t)$$

Look at frequency difference terms

$$P \approx -J_1(\beta)\frac{M}{2}\sin((\Omega-\gamma)t+\phi) - J_1(\beta)\frac{M}{2}\sin((-\Omega+\gamma)t+\phi) + J_1(\beta)\frac{M}{2}\sin((-\Omega-\gamma)t+\phi) + J_1(\beta)\frac{M}{2}\sin((\Omega+\gamma)t+\phi)$$

$\sin(-\theta) = -\sin(\theta)$ --- $\sin(\alpha \pm \beta) = \sin(\alpha)\cos(\beta) \pm \cos(\alpha)\sin(\beta)$

$$P \approx -J_1(\beta)\frac{M}{2}\sin((\Omega-\gamma)t+\phi) + J_1(\beta)\frac{M}{2}\sin((\Omega-\gamma)t-\phi) - J_1(\beta)\frac{M}{2}\sin((\Omega+\gamma)t-\phi) + J_1(\beta)\frac{M}{2}\sin((\Omega+\gamma)t+\phi)$$

$$P \approx J_1(\beta)\frac{M}{2}[\{-\sin((\Omega-\gamma)t)\cos(\phi) - \cos((\Omega-\gamma)t)\sin(\phi) + \sin((\Omega-\gamma)t)\cos(\phi) - \cos((\Omega-\gamma)t)\sin(\phi)\} +$$

$$\{-\sin((\Omega+\gamma)t)\cos(\phi) + \cos((\Omega+\gamma)t)\sin(\phi) + \sin((\Omega+\gamma)t)\cos(\phi) + \cos((\Omega+\gamma)t)\sin(\phi)\}]$$

$$P \approx J_1(\beta)\frac{M}{2}[-2\cos((\Omega-\gamma)t)\sin(\phi) + 2\cos((\Omega+\gamma)t)\sin(\phi)]$$

Using a mixer select difference frequency and small angle - - $\sin(\phi) = \phi$

$$P \approx -J_1(\beta)M\cos((\Omega-\gamma)t) * \phi = \delta L * \{-J_1(\beta)M\cos((\Omega-\gamma)t)\}$$

Error Signal = $\delta L * \{-J_1(\beta)M\cos((\Omega-\gamma)t)\}$

Note that the error signal is proportional to the phase error in the cavity and that the error signal goes to zero when the phase error goes to zero (cavity on resonance). Also, when the phase error is positive or negative (too short/too long) the error signal is also positive or negative. This error signal can therefore be amplified and connected to a length-adjusting servomechanism to lock the cavity (keep it on resonance) and thereby complete the feedback control loop.

References

[1] Black, Eric. *Notes on the Pound-Drever-Hall Technique*. LIGO-T980045-00 – D
http://www.ligo.caltech.edu/docs/T/T980045-00.pdf

[2] Drever, R.W.P., *et al*., Appl. Phys. B 31, 97 (1983)

[3] Evans, M., *et al*., *Lock Acquisition Of A Gravitational Wave Interferometer.* Optics Letters, 27, 598 (2001)

[4] Saleh, B.E.A., and Teich, M.C., Fundamentals Of Photonics.
(Wiley-Interscience Publications, New York, New York, 1991).

[5] Adhikari, Rana, *et al*., *Input Optics Final Design.* LIGO-T980009-01-D
http://www.ligo.caltech.edu/docs/T/T980009-01.pdf